Jordan Journal of Physics

ARTICLE

DFT Study of the π - π Interaction between Graphene and Liquid Crystal Molecules for the Charge Transfer Applications

Tikaram, Yogesh Kumar and Narinder Kumar

Department of Physics, School of Applied & Life Sciences, Uttaranchal University, Dehradun, Uttarakhand-248007, India.

Doi: https://doi.org/10.47011/18.3.1

Received on: 20/04/2023; Accepted on: 05/05/2024

Abstract: As the LC and GP sheets meet, the ionization potential, HOMO-LUMO gap, and cosmo area of the whole dimer (LC+GP) all drop. Every LC engages in a parallel plane (armchair) or diagonal cross-section interaction with the GP. Benzene-based liquid crystals interact strongly with graphene, whereas cyclohexane-based liquid crystals interact only weakly. Liquid crystal dimers based on benzene interact negatively with graphene. Liquid crystals composed of oxygen and nitrogen atoms exhibit interactions with graphene. Whereas nitrogen atom-based liquid crystals very faintly interact with graphene, oxygen atom-based liquid crystals do so energetically. In contrast to the nitrogen atom-based liquid crystal, the oxygen atom-based liquid crystal dimer displays a more impressive dipole moment. The strongest dipole moment is observed for the liquid crystal containing both nitrogen and oxygen atoms. The graphene sheet twisted in all the dimers, and all the liquid crystal benzene rings exhibit the π - π interaction with the graphene at a distance of \sim 3.5Å. The cyclohexane ring and the terminal group of the liquid crystal interact with graphene at a distance of \sim 2.5Å, but they do not show π -stacking.

Keywords: Graphene, Liquid crystal, Molecular interaction, π - π stacking, Density Functional Theory (DFT).

Introduction

Graphene [1] has a hexagonal arrangement of carbon atoms and acquires a 2D crystalline solid structure in a planar form [2]. The sp² hybridization of carbon atoms in graphene is responsible for the high charge carrier mobility, excellent mechanical flexibility, and very high thermal conductivity; hence, graphene has a wide range of applications in optical devices [3]. Owing to its large surface-to-volume ratio, graphene is particularly well suited for ultracapacitor and chemical sensor applications [4]. Its transparency and low-cost availability make it attractive for use in organic lightemitting diodes (OLEDs), touchscreen displays, solar cells Graphene-based [5]. photodetectors operate at a very high frequency [6]. Graphene has a conical electronic bandgap structure that lies between the valence and conduction bands [7]. The valence conduction bands overlap slightly, classifying it as a zero-bandgap semimetal. Graphene is one of the allotropes of carbon made of a single layer of carbon atoms arranged in a hexagonal lattice. Besides graphene, other allotropes of carbon are diamond, fullerene, charcoal, and carbon nanotubes. Graphene behaves as a good conductor of heat and electricity and is capable of light absorption. Graphene is about 200 times stronger than steel [9]. Graphene-based liquid exhibit high-speed electro-optic crystals switching. Their interaction with graphene is governed by π - π electron stacking. interactions between liquid crystals and graphene through π - π electron stacking establish a planar

Corresponding Author: Narinder Kumar Email: knarinder 7@gmail.com

arrangement of the liquid crystal in graphenebased cells. Graphene-based liquid crystals actively exhibit a nematic phase under the effect of an electric field. Basu et al. reported that π - π interaction of LC with GP gives rise to the physical and optical properties of dimers. The LC reduces the free ion concentration by an iontrapping process after the communication of LC and GP; the present work also reveals an enhancement in the ionization potential of the dimer [9]. The birefringence of liquid crystals predicts a new technique to visualize domain and grain boundaries of graphene. The liquid crystal and graphene have strong epitaxial interactions, and liquid crystals have planar orientation along with graphene [10]. The anchoring forces align liquid crystals and graphene in the planar configuration. Shehzad et al. reported that the nematic liquid crystal on graphene usually makes six random conformations [11]. The nematic and smectic type liquid crystals impose planar alignment on the graphene surface. The decreased free ion concentration in the dimer (LC+GP) reduces the rotational viscosity that is responsible for the electro-optic switching or faster response [12]. In this work, we are using rod-like, nematic-phase LC molecules. The interaction of LC and GP affects such parameters as ionization potential, HOMO-LUMO gap, COSMO area, COSMO volume, and dipole moment of the dimer. Shen et al. demonstrated that doping LCs with GP enhances the physical properties of the dimer, particularly the dipole moment, because free ions in the LC are trapped by GP, thereby lowering the threshold voltage [13]. Mrukiewicz et al. reported that the strong π -π interaction between 5CB LC and GP makes this combination suitable for applications in LC modulators, filters, isotropic LC displays, and smart windows [14]. Fischer et al. reported that 5CB LC adsorbs onto GP in the armchair conformation; the present work also reveals that 5CB LCs interact with GP in the armchair conformation [15]. Basu et al., Kumar et al., and Lapanik et al. reported that the strong π - π interaction of LCs with GP enhances the dipole moment; the present work also reveals a dipole moment increase of H5CBP LC because it transfers the maximum charge to GP [16-17].

Computational Methodology

Graphene and liquid crystal molecules are optimized by the Gaussian 09 software package

[18] with the help of DFT LC-BLYP method [19-20] and 6-31G basis set [21]. All dimers were optimized by seven DFT methods, and we have considered only the LC-BLYP minimum energy conformations of the GP and LC. All dimers were generated under free optimization (where coordinates were not fixed). Under the free optimization, all monomers (GP & LC) randomly interacted with each other and produced one minimum energy conformation. The total energy (ΔE) of the dimer (LC+GP) was calculated by the formula given below [22]

$$\Delta E = E_{el} + E_{rep} + E_{pol} + E_{disp}$$

where E_{el} , E_{rep} , E_{pol} , and E_{disp} represent the attractive electrostatic, short-range repulsion, polarization, and dispersion energy, respectively.

Results and Discussion

In this work, we confirm that LCs interact with GP primarily through parallel stacking. All studied LCs are polar, which accounts for the high dipole moments observed in the dimers. The molecular weight of the dimers remains however, unaffected after interaction; ionization potential, COSMO area, and the highest occupied molecular orbital (HOMO) and the lowest unoccupied molecular orbital (LUMO) gap decrease for all dimers upon interaction between GP and LC. The COSMO volume of the dimers either increases or decreases depending on the LC type. All LC dimers exhibit positive interaction energy, as adsorption occurs in different conformations. Among the studied LCs, H5CBP transfers the maximum charge to GP, making it most suitable charge-transfer applications. disubstituted diphenylacetylenes, PCH, and 7O LC also transfer appreciable charge to GP; however, H5CBP remains the most effective.

CCH5 (5-Cyclohexylcyclohexane-1,3-dione) LC & GP

Where $[D-(M_1+M_2)]:-[Dimer energy \{LC+GP\} - (Monomer energy (M_1) \{LC\} + Monomer (M_2) energy \{GP\})]$

The GP and CCH5 LC interact via parallelplane stacking. As shown in Fig. 1 and Table 1, this conformation reduces the ionization potential, HOMO–LUMO gap, dipole moment, and COSMO area, while increasing both the total energy and COSMO volume of the dimer. Because of its two cyclohexane rings, this LC

exhibits modest interaction energy with the GP. Compared to the benzene ring, the cyclohexane ring shows weaker contact. Although the cyclohexane ring has a chair conformation, the benzene ring has a planar shape. A benzene ring contains carbon atoms that have undergone sp2 hybridization, whereas a cyclohexane ring has sp3 hybridization. Their respective melting and boiling points, as well as molecular masses, are different. The benzene molecule has delocalized pi-electron clouds, but the cyclohexane ring does not. Sigma bonds and pi delocalized electrons distinguish cyclohexane as an aliphatic

compound and benzene as an aromatic one. Because of the electron being trapped, the CCH5 LC transfers the least amount of charge to graphene. Due to the lack of interaction in CCH5 LC, the GP sheet became somewhat distorted. At a distance of 2.85, the hydrogen atom of GP interacts with the nitrogen atom of the cyano group. At a minimum distance of 2.56, the first cyclohexane ring interacts with the general potential. At a distance of 2.54, the carbon atom of GP interacts with the second hydrogen atom of the cyclohexane ring. At a distance of 2.52, the tail of the LC contacts the GP surface.

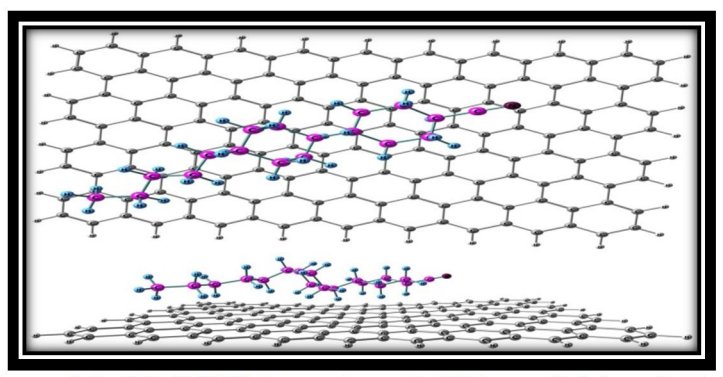


FIG. 1. Side and top views of the LC (CCH5) interacting with GP in parallel (armchair) stacking. The dielectric and optical anisotropies of all CCH molecules are much lower than those of the corresponding CB or PCH molecules. CCH-4, in particular, can serve as a liquid-crystalline solvent in spectroscopic applications. In general, CCH liquid crystals exhibit low birefringence and high negative dielectric anisotropy, making them suitable for such use.

TABLE 1. Total energy, dipole moment, ionization potential, HOMO–LUMO gap, molecular weight, COSMO area, and COSMO volume of the CCH5–GP dimer shown in Fig. 1.

CCH5_GP	Monomer (LC)	Monomer (GP)	Dimer (LC+GP)	Difference [D-(M ₁ +M ₂)]
Total Energy (a.u.)	-756.78194	-5812.3749	-6551.2975	-17.8593
Dipole moment (Debye)	4.60	0.00	1.39	-3.21
Ionization potential (eV)	10.83	3.76	4.86	-9.73
HOMO-LUMO gap (eV)	6.59	0.16	2.15	-4.60
Molecular Weight	261.44	1859.94	2121.39	0.00
Cosmo Area (Å) ²	330.04	1229.95	1322.51	-237.48
Cosmo Volume (Å) ³	376.35	1776.96	2169.04	15.73

P.P'-disubstituted diphenylacetylenes LC & GP

The P.P'-disubstituted diphenylacetylenes LC [25] interacts diagonally with tGP in the parallel plane. The dipole moment, ionisation potential, HOMO-LUMO gap, and COSMO area in this dimer diminish when the GP and LC engage with one another in the parallel plane diagonal configuration, as illustrated in Fig. 2 and Table 2, while the total energy and COSMO volume rise. It is appropriate for solar cell applications since the P.P'-disubstituted diphenylacetylenes LC deliver roughly the same amount of charge to the graphene. The P.P'-disubstituted

diphenylacetylenes LC display the interaction; however, the tail of LC does not express stacking, which causes the GP sheet to twist. At a distance of 2.63, the CH3 group bonded to the oxygen atom displays interactions with the GP. At a distance of 3.44 from GP, the oxygen atom interacts with it. At a distance of 3.41, the carbon atom of GP. At a distance of 3.38, the other benzene in LC interacts with the carbon atom in GP. At a distance of 2.65, the tail of the LC contacts with GP.

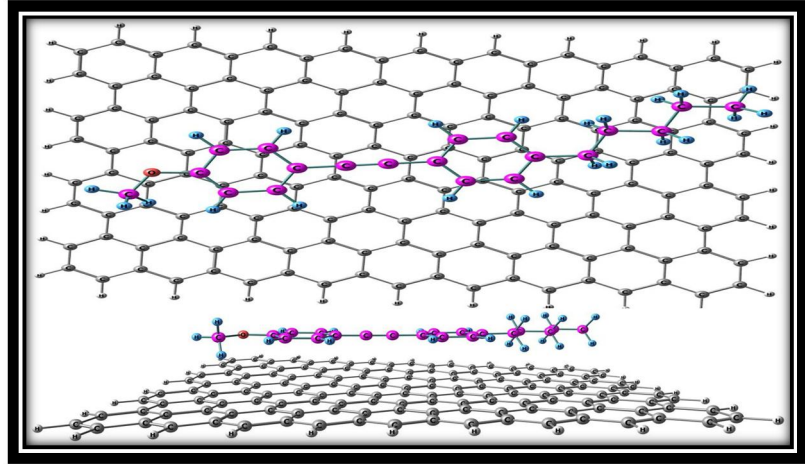


FIG. 2. Side and top view showing the interaction of LC (P.P'-disubstituted diphenylacetylenes) with GP in parallel (armchair) stacking. The electronic properties of graphene stacks depend on the stacking order and the number of layers. The interaction of molecules with graphene can be tuned by doping the graphene sheet with dopant atoms, which regulate the van der Waals forces exerted on adsorbed molecules. Functionalization of graphene typically occurs through π - π interactions between the graphene surface and other moieties. Graphene, a one-atom-thick allotrope of carbon, exhibits unique two-dimensional Dirac-like electronic excitations. The behavior of Dirac electrons in graphene can be modulated by external electric and magnetic fields, or by altering the sample's geometry and topology.

TABLE 2. Total energy, dipole moment, ionization potential, HOMO-LUMO gap, molecular weight, COSMO area, and COSMO volume of the dimer shown in Fig. 2.

CODITIO dired, dila CODITIO	Cosino area, and Cosino volume of the anner shown in 11g. 2.					
P.P' D-D LC_ GP	Monomer (LC)	Dimer (LC+GP)	Difference $[D-(M_1+M_2)]$			
Total Energy (a.u.)	-847.73885	-6642.2641	-17.8496			
Dipole moment (Debye)	1.58	1.55	-0.03			
Ionization potential (eV)	7.93	4.84	-6.85			
HOMO-LUMO gap (eV)	6.54	2.16	-4.54			
Molecular Weight	278.39	2138.33	0.00			
COSMO Area (Å) ²	358.23	1307.48	-280.7			
COSMO Volume (Å) ³	372.49	2152.15	2.7			

5CB LC & GP

GP and the 5CB (4-Cyano-4'-pentylbiphenyl) LC [26–27] interact in the parallel plane. When GP and LC engage on the parallel plane configuration depicted in Fig. 3 and Table 3, the ionisation potential, HOMO-LUMO gap, COSMO volume, dipole moment, and COSMO area decrease, while the total energy and COSMO volume rise. According to Basu *et al.*, the physical and optical characteristics of dimers are the result of the LC and GP interacting negatively. After communicating with GP, the LC uses an ion-trapping mechanism to lower the concentration of free ions [22–23]. The contact

causes the GP's zero dipole moment to grow through an ion-trapping mechanism (present work). Because 5CB LC displays the interaction while the tail of LC does not, the GP sheet is twisted. Because of its small charge transfer to graphene, the 5CB LC is not suited for solar applications. At a distance of 3.21, the hydrogen atom of GP interacts with the nitrogen atom of the cyano group. At a distance of 2.99, the benzene from the cyano group side interacts with GP. At a distance of 3.17, the second benzene reacts with GP. At a distance of 2.61, the tail of the LC interacts with GP.

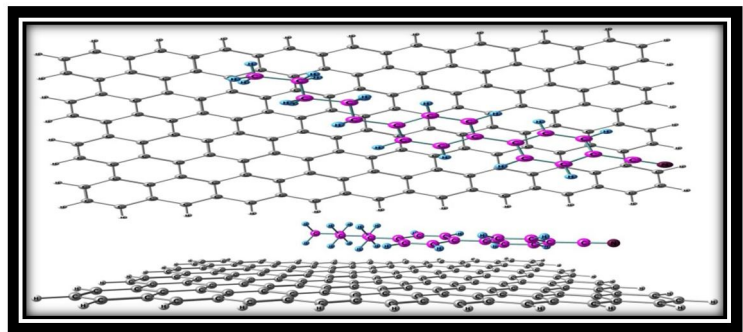


FIG. 3. Side and top views showing the interaction of LC (5CB) with GP in parallel (armchair) stacking. Density functional theory (DFT) was used to investigate the stable adsorption geometries of the liquid crystal molecule 5CB on a graphene sheet. Results indicate that the insertion reaction is likely spontaneous and irreversible, suggesting a potential pathway for tuning both liquid crystal behavior and graphene properties. The two-dimensional honeycomb structure of graphene interacts with the benzene rings of the LC through π - π electron stacking. The homeotropic alignment of the 5CB molecule on monovacancy graphene differs from its preferred planar orientation on pristine graphene.

Table 3. Total energy, dipole moment, ionization potential, HOMO-LUMO gap, molecular weight, COSMO area, and COSMO volume of the dimer shown in Fig. 3.

		<u> </u>	
5CB_ GP	Monomer (LC)	Dimer (LC+GP)	Difference [D-(M ₁ +M ₂)]
Total Energy (a.u.)	-749.588844	-6544.1145	-17.8492
Dipole moment (Debye)	5.69	2.29	-3.40
Ionization potential (eV)	9.00	4.86	-7.90
HOMO-LUMO gap (eV)	8.22	2.15	-6.23
Molecular Weight	249.35	2109.29	0.00
COSMO Area (Å) ²	319.15	1301.10	-248
COSMO Volume (Å) ³	336.56	2138.71	25.19

PCH5 (4-(trans-4-Pentylcyclohexyl)benzonitrile) LC & GP

GP and the PCH5 trans-4-pentyl-(4-cyanophenyl)-cyclohexane LC [28-29] interact on a parallel plane. When GP and LC interact with one another in A parallel plane configuration, as illustrated in Fig. 4 and Table 4, the ionisation potential, dipole moment, HOMO-LUMO gap, and COSMO area drop while the COSMO volume and total energy rise.

Because it transfers more charge to graphene, the PCH5 LC is superior to the 5CB LC. Since the PCH5 LC displays the π - π interaction while the cyclohexane ring and tail of the LC do not, the GP sheet is somewhat bent. At a distance of 3.01, the cyano group's nitrogen atom interacts with GP. At a distance of 2.96, the benzene ring interacts with GP. The cyclohexane reacts with GP at a distance of 2.60. The alkyl chain contacts GP at a distance of 2.71.

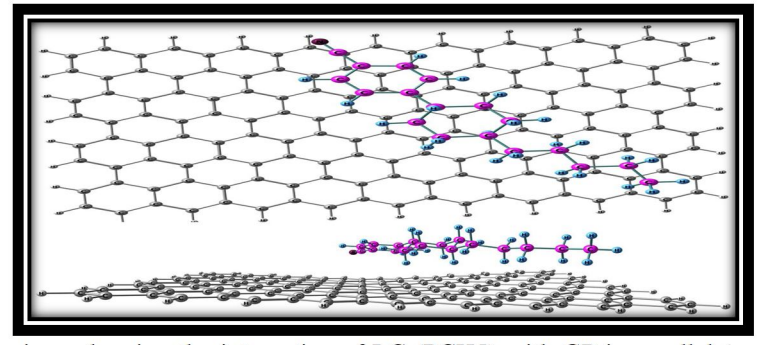


FIG. 4. Side and top views showing the interaction of LC (PCH5) with GP in parallel (armchair) stacking. The two-dimensional graphene honeycomb structure interacts with the liquid crystal's (LC) benzene rings through π – π electron stacking. The results indicate that the insertion reaction is likely spontaneous and irreversible, offering a potential pathway for controlling both liquid crystal behavior and graphene properties. PCH5 is a rod-like liquid crystal with a nematic–isotropic phase transition at 327.6 K. At a distance of 3.01, the nitrogen atom of the cyano group interacts with GP.

TABLE 4. Total energy, dipole moment, ionization potential, HOMO-LUMO gap, molecular weight, COSMO area, and COSMO volume of the dimer shown in Fig. 4.

		0	
PCH_GP	Monomer (LC)	Dimer (LC+GP)	Difference [D-(M ₁ +M ₂)]
Total Energy (a.u.)	-753.18566	-6547.7126	-17.8479
Dipole moment (Debye)	5.42	5.06	-0.36
Ionization potential (eV)	9.74	4.93	-8.57
HOMO-LUMO gap (eV)	8.48	2.29	-6.35
Molecular Weight	255.40	2115.34	0.00
COSMO Area (Å) ²	324.82	1314.72	-240.05
COSMO Volume (Å) ³	354.51	2145.26	13.79

6O.2 or 6O.5 LC & GP

The interaction between GP and 6O.5 {4-5-Alkyl-N-(4-6-Alkyloxy-Benzylidene)-Anilines} LC [30] takes the form of a letter V. When the GP and LC interact in the form of a letter V, as illustrated in Fig. 5 and Table 5, the ionisation potential, HOMO-LUMO gap, cosmo volume, cosmo area, and dipole moment drop, while the total energy increases. Graphene does not receive charges from the 6O.5 LC at a suitable pace. Due to the π - π interaction present in 6O.5 LC, the GP sheet twisted. At a distance of 2.72,

the nitrogen atom's side of the LC tail interacts with GP. At a distance of 2.78, the benzene interacts with GP on the side of the nitrogen atom. At a distance of 3.43, the nitrogen atom of the bridging group interacts with the carbon atom of GP. At a distance of 2.62, the side of benzene that interacts with GP connects with the oxygen atom. The oxygen atom of LC interacts with the carbon atom at a distance of 4.70Å. The tail of the oxygen atom side LC interacts with GP at a distance of 2.68Å.

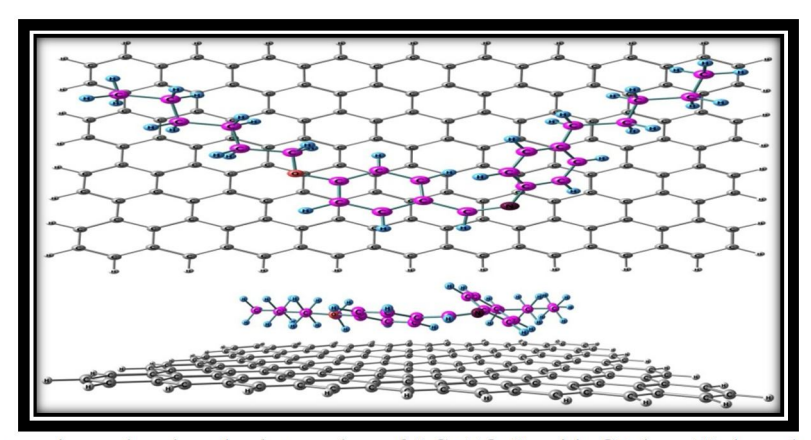


FIG. 5. Side and top views showing the interaction of LC (60.5) with GP in a V-shaped conformation. This liquid crystal flows like a liquid but maintains molecular alignment in a crystal-like manner, producing characteristic textures observable under a microscope. 60.5 LC has a low melting point, high boiling point, high viscosity, and low surface tension. It also exhibits high dielectric anisotropy, meaning its dielectric constant varies along different molecular axes. These properties make it useful in applications such as liquid crystal displays (LCDs), thermometers, and mood rings. Due to the π - π interaction present in 60.5 LC, the GP sheet is twisted. At a distance of 2.72, the nitrogen atom's side of the LC tail interacts with GP.

Table 5. Total energy, dipole moment, ionization potential, HOMO-LUMO gap, molecular weight, COSMO area, and COSMO volume of the dimer shown in Fig. 5.

6O.5_ GP	Monomer (LC)	Dimer (LC+GP)	Difference [D-(M ₁ +M ₂)]
Total Energy (a.u.)	-1060.88216	-6855.3974	-17.8596
Dipole moment (Debye)	3.78	2.19	-1.59
Ionization potential (eV)	8.16	4.85	-7.07
HOMO-LUMO gap (eV)	6.82	2.15	-4.83
Molecular Weight	351.53	2211.47	0.00
COSMO Area (Å) ²	444.56	1335.02	-339.49
COSMO Volume (Å) ³	482.40	2250.39	-8.97

70.5 LC & GP

In parallel plane stacking, GP and 70.5 {4-5-Alkyl-N-(4-7-Alkyloxy-Benzylidene)-Anilines} LC [31-32] interact. As GP and LC interact, as illustrated in Fig. 6 and Table 6, the ionisation potential, HOMO-LUMO gap, dipole moment, and COSMO area drop, while the total energy and COSMO volume rise. Compared to 60.5 LC, 70.5 has a greater charge transfer rate. Due to the π - π interaction displayed by 70.5 LC, the

GP sheet becomes twisted. At a distance of 2.62, the benzene interacts with GP from the side of the oxygen atom. At a distance of 2.55, the oxygen atom's side of the liquid crystal tail contacts with GP. At a distance of 2.90, the hydrogen atom in the bridging group interacts with GP. At a distance of 3.56, the second benzene reacts with GP. At a distance of 2.65, the tail of the LC contacts with GP.

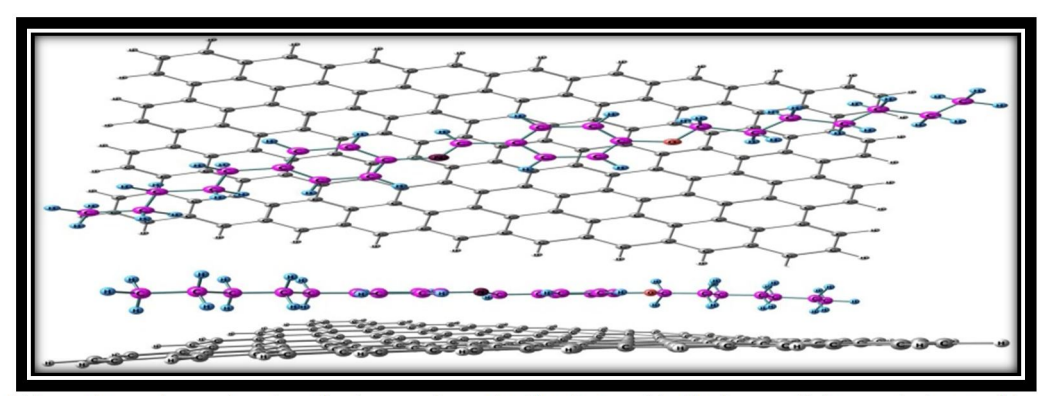


FIG. 6. Side and top views showing the interaction of LC (70.5) with GP in parallel (armchair) stacking. The 4-5-Alkyl-N-(4-7-Alkyloxy-Benzylidene)-Anilines belong to the benzylidene aniline family, characterized by an alkyl group and an alkoxybenzylidene group attached to an aniline core. Their properties depend strongly on the length of the alkyl and alkoxy chains, which influence phase transition behavior. These compounds have also been used to design liquid crystal assemblies through hydrogen-bonding interactions. In this work, the π - π interaction of 70.5 LC with GP causeS the graphene sheet to twist. At a distance of 2.62, the benzene interacts with GP from the side of the oxygen atom.

Table 6. Total energy, dipole moment, ionization potential, HOMO-LUMO gap, molecular weight, COSMO area, and COSMO volume of the dimer shown in Fig. 6.

7O_GP	Monomer (LC)	Dimer (LC+GP)	Difference [D-(M ₁ +M ₂)]
Total Energy (a.u.)	-1100.06930	-6894.5935	-17.8507
Dipole moment (Debye)	3.08	2.50	-0.58
Ionization potential (eV)	8.17	4.86	-7.07
HOMO-LUMO gap (eV)	7.05	2.15	-5.06
Molecular Weight	365.55	2225.49	0.00
COSMO Area (Å) ²	477.47	1358.88	-348.54
COSMO Volume (Å) ³	502.06	2309.60	30.58

4-4' Disubstituted Biphenyls LC & GP

GP and the 4-4' disubstituted biphenyls LC [33] engage in a parallel plane stacking interaction. During the interaction seen in Fig. 7 and Table 7, the dimer's ionisation potential, dipole moment, HOMO-LUMO gap, COSMO volume, and COSMO area drop as the total energy increases. The 4-4' disubstituted biphenyls LC shows the π - π interaction, which

causes the GP sheet to twist. The 4-4' disubstituted biphenyls do not transfer charges to graphene at a sufficient rate. At a distance of 3.21, the cyano group's nitrogen atom interacts with GP; at 3.26, the benzene ring adjacent to the cyano group interacts with GP; at 2.89, the second benzene ring interacts with GP; at 3.28, the oxygen atom interacts with GP; and at 2.53, the LC tail interacts with GP.

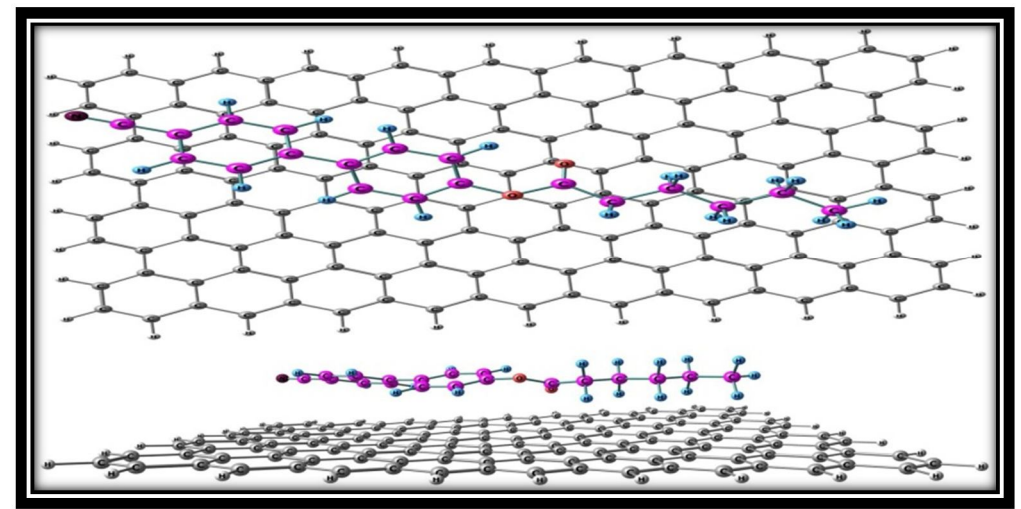


FIG. 7. Side and top showing the interaction of LC (4-4' disubstituted biphenyls) with GP in parallel (armchair) stacking. The 4-4' disubstituted biphenyls represent a homologous series of liquid crystals derived from the biphenyl moiety. One of the most widely studied members of this series is 5CB (4-cyano-4'-pentylbiphenyl), a nematic liquid crystal known for its phase transition behavior. Soluble, chemically oxidized graphene or graphene oxide sheets can form chiral liquid crystals with a twist-grain-boundary structure. Moreover, the tilt angle of nematic liquid crystals can be influenced by the number of graphene layers present. These biphenyl-based LC molecules can insert into monovacancy graphene, potentially providing a new pathway for tuning both liquid crystal alignment and graphene properties.

TABLE 7. Total energy, dipole moment, ionization potential, HOMO-LUMO gap, molecular weight, COSMO area, and COSMO volume of the dimer shown in Fig. 7.

4-4'Disubstituted Bi GP	Monomer (LC)	Dimer (LC+GP)	Difference [D-(M ₁ +M ₂)]
Total Energy (a.u.)	-937.68956	-6732.2152	-17.8492
Dipole moment (Debye)	5.86	2.91	-3.67
Ionization potential (eV)	9.11	4.85	-8.02
HOMO-LUMO gap (eV)	8.47	2.14	-6.49
Molecular Weight	293.36	2153.30	0.00
COSMO Area (Å) ²	353.02	1307.96	-275.01
COSMO Volume (Å) ³	370.19	2147.09	-0.06

MBA5 or APAPA5 LC & GP

In parallel plane stacking, GP and MBA5 (panisylidene p-aminophenylacetate) LC [34] interact. As GP and LC interact, as demonstrated in Fig. 8 and Table 8, the ionisation potential, HOMO-LUMO gap, COSMO volume, dipole moment, and COSMO area drop, while the total energy increases. Because of the three oxygen and one nitrogen atoms in this LC, this dimer has the largest dipole moment. The MBA5 LC has a lower maximum charge transfer rate to GP. Due to the π - π interaction that MBA5 LC displays,

the GP sheet becomes twisted. At a distance of 3.86, the oxygen atom with the CH3 group interacts with GP. At a distance of 2.88, the benzene from the side of a single oxygen atom interacts with GP. At a distance of 3.04, the hydrogen atom of the bridging group interacts with the carbon atom of GP. At a distance of 3.21, the other benzene in the LC interacts with GP. At a distance of 2.55 from GP, the oxygen atom interacts with it. The alkyl chain contacts GP at a 2.62 distance.

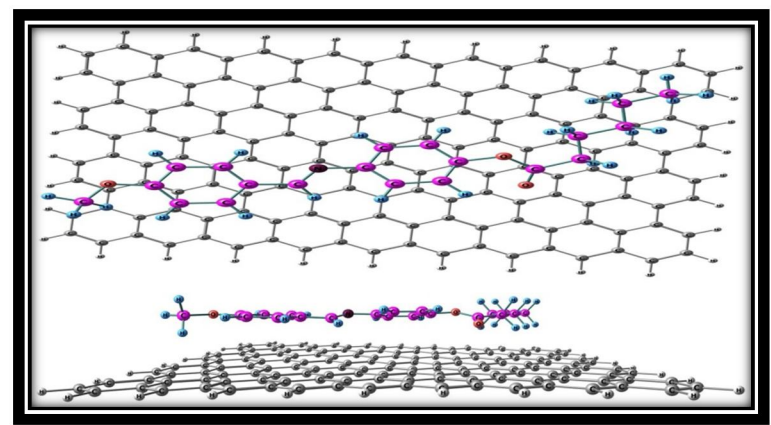


FIG. 8. Side and top views showing the interaction of LC (MBA5) with GP in parallel (armchair) stacking. This liquid crystal exhibits a characteristic texture observable under a microscope. Its optical properties depend on molecular orientation, which can be controlled by electric or magnetic fields. MBA5 has a low melting point and a high boiling point, along with high viscosity and low surface tension. It also exhibits high dielectric anisotropy, meaning its dielectric constant varies along different molecular axes.

TABLE 8. Total energy, dipole moment, ionization potential, HOMO-LUMO gap, molecular weight, COSMO area, and COSMO volume of the dimer shown in Fig. 8.

,		\mathcal{L}	
MBA5_ GP	Monomer (LC)	Dimer (LC+GP)	Difference [D-(M ₁ +M ₂)]
Total Energy (a.u.)	-1053.10434	-6847.6278	-17.8514
Dipole moment (Debye)	2.13	1.11	-1.02
Ionization potential (eV)	8.30	4.85	-7.21
HOMO-LUMO gap (eV)	7.35	2.17	-5.34
Molecular Weight	325.40	2185.34	0.00
COSMO Area (Å) ²	390.57	1307.50	-313.02
COSMO Volume (Å) ³	406.83	2180.53	-3.26

MBC5 or PMBAB5 LC & GP

In parallel plane stacking, GP and the MBC5 {N-(p-methoxybenzylidene)-p-aminobenzonitrile} LC [35] interact. As illustrated in Fig. 9 and Table 9, when GP and LC interact with one another, the ionisation potential, dipole moment, HOMO-LUMO gap, and COSMO area drop, while the total energy and COSMO volume rise. The MBC5 LC displays the π - π interaction, which causes the GP sheet to be somewhat bent. Moreover, the

MBC5 LC does not transfer charges to GP at an appropriate pace. At a distance of 3.11, the nitrogen atom of the cyano group interacts with the GP. At a distance of 3.51, the benzene ring from the cyano group interacts with GP. At a distance of 2.69, the hydrogen atom in the bridging group interacts with GP. At a distance of 2.88, the other benzene ring interacts with GP. At a distance of 3.85 from GP, the oxygen atom interacts with it. The alkyl chain contacts GP at a 2.61 distance.

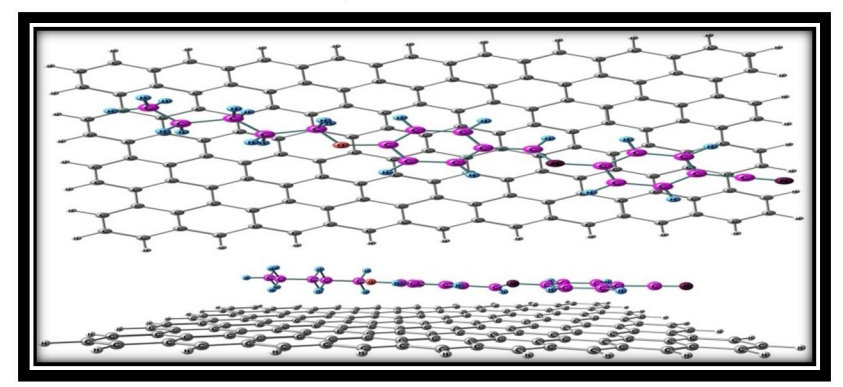


FIG. 9. Side and top views showing the interaction of LC (MBC5) with GP at parallel (armchair) stacking. The nitrogen atom of the cyano group interacts with GP at 3.11, the benzene ring adjacent to the cyano group at 3.51, the hydrogen atom in the bridging group at 2.69, and the second benzene ring at 2.88.

TABLE 9. Total energy, dipole moment, ionization potential, HOMO-LUMO gap, molecular weight, COSMO area, and COSMO volume of the dimer shown in Fig. 9.

		0	
MBC5_GP	Monomer (LC)	Dimer (LC+GP)	Difference [D-(M ₁ +M ₂)]
Total Energy (a.u.)	-917.79444	-6712.3187	-17.8506
Dipole moment (Debye)	7.53	3.54	-3.99
Ionization potential (eV)	8.67	4.87	-7.56
HOMO-LUMO gap (eV)	8.25	2.14	-6.27
Molecular Weight	292.37	2152.32	0.00
COSMO Area (Å) ²	364.04	1313.28	-280.71
COSMO Volume (Å) ³	373.92	2160.48	9.60

H5CBP LC & GP

GP and the H5CBP "eight 4,4'-disubstituted biphenyls" LC engage in parallel plane stacking interaction. As shown in Fig. 10 and Table 10, the interaction causes the ionization potential, HOMO-LUMO gap, and COSMO area to drop while the dipole moment, COSMO volume, and total energy rise. The H5CBP LC displays the π - π interaction; however, the tail of the LC does not express stacking, which causes the GP sheet to twist. The H5CBP LC transfers the most charge to the GP, making it ideal for applications

in solar cells or electronic charge transfer. The H5CBP LC has a high concentration of free ions. At a distance of 3.19, the nitrogen atom of LC interacts with the carbon atom of GP. At a distance of 3.10, the benzene ring from the cyano group interacts with GP. At a distance of 2.98, the other benzene ring interacts with GP. At a distance of 3.61, the oxygen atom of the LC interacts with GP. At a distance of 2.49, the tail of the LC contacts GP. The oxygen atom interacts with the carbon atom at the tail's end at a distance of 3.36.

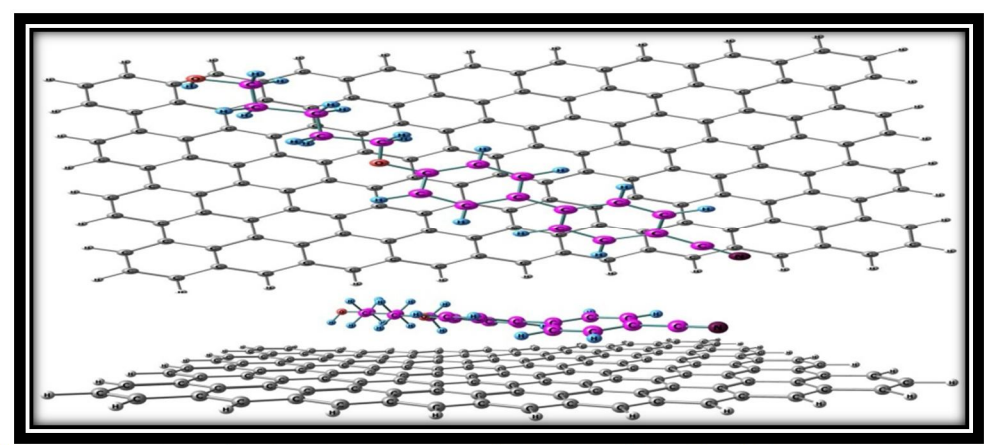


FIG. 10. Side and top views showing the interaction of LC (H5CBP) with GP in parallel (armchair) stacking. H5CBP LC transfers the most to GP, making it ideal for solar cell and electronic charge-transfer applications. The H5CBP LC has a high concentration of free ions. At a distance of 3.19, the nitrogen atom of LC interacts with the carbon atom of GP. At a distance of 3.10, the benzene ring from the cyano group interacts with GP.

TABLE 10. Total energy, dipole moment, ionization potential, HOMO-LUMO gap, molecular weight, COSMO area, and COSMO volume of the dimer shown in Fig. 10.

H5CBP_GP	Monomer (LC)	Dimer (LC+GP)	Difference [D-(M ₁ +M ₂)]
Total Energy (a.u.)	-899.67823	-6694.2072	-17.8459
Dipole moment (Debye)	6.52	7.55	1.03
Ionization potential (eV)	8.64	4.89	-7.51
HOMO-LUMO gap (eV)	7.80	2.14	-5.82
Molecular Weight	281.35	2141.29	0.00
COSMO Area (Å) ²	342.59	1310.54	-262.00
COSMO Volume (Å) ³	357.96	2136.21	1.29

5OCB LC & GP

GP interacts with the 5OCB (pentyloxycyanobipheny) LC [36–39] in parallel plane stacking. As shown in Fig. 11 and Table 11, the interaction causes decreases in ionisation potential, HOMO-LUMO gap, dipole moment, and COSMO area, while the COSMO volume and total energy rise. In contrast to H5CBP LC, which has two oxygen and one nitrogen atom, 5OCB LC has just one oxygen and one nitrogen atom, hence it does not have a good charge-

transfer rate. Oxygen is more electronegative than nitrogen, which affects the interaction. Due to the π - π interaction displayed by 5OCB LC, the GP sheet becomes slightly bent. Key interactions include: the nitrogen atom of the cyano group with GP at a distance of 3.21; the benzene ring adjacent to the cyano group at a distance of 3.30; the second benzene ring on the oxygen side at a distance of 2.85; the LC tail at a distance of 2.52; and the oxygen atom at a distance of 3.88.

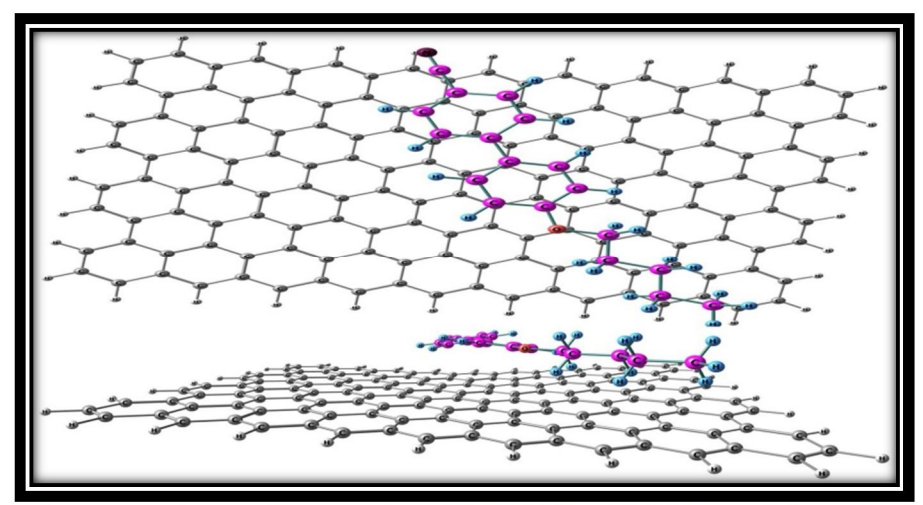


FIG. 11. Side and top views showing the interaction of LC (50CB) with GP in parallel (armchair) stacking. Due to the - interaction exhibited by 50CB LC, the GP sheet is slightly bent. At a distance of 3.21, the cyano group's nitrogen atom interacts with GP. At a distance of 3.30, the benzene ring from the cyano group interacts with GP. At a distance of 2.85, the second benzene ring from the side of the oxygen atom interacts with GP. At a distance of 2.52, the tail of the LC contacts with GP. At a distance of 3.88 from GP, the oxygen atom interacts with it.

TABLE 11. Total energy, dipole moment, ionization potential, HOMO-LUMO gap, molecular weight, COSMO area, and COSMO volume of the dimer shown in Fig. 11.

5OCB_ GP	Monomer (LC)	Dimer (LC+GP)	Difference [D-(M ₁ +M ₂)]
Total Energy (a.u.)	-824.63521	-6619.1634	-17.8467
Dipole moment (Debye)	6.24	5.28	-0.96
Ionization potential (eV)	8.63	4.94	-7.45
HOMO-LUMO gap (eV)	7.78	2.30	-5.64
Molecular Weight	265.35	2125.29	0.00
COSMO Area (Å) ²	331.53	1314.41	-247.07
COSMO Volume (Å) ³	345.17	2124.85	2.72

The negative interaction energy indicates that all the LCs are adsorbed on GP. Table 12 compares the interaction energies of all dimers in decreasing order. Among them, H5CBP LC is perfectly adsorbed on GP and has the lowest (least negative) interaction energy, meaning it

transfers the maximum charge to GP, making it ideal for charge-transfer applications.

6O.5 > CCH5 > MBA5 > 7O > MBC5 > P.P'-disubstituted diphenylacetylenes > 5CB > 4-4'disubstituted biphenyls > PCH5 > 5OCB > H5CBP

TABLE 12.	Comparison of	of the interaction	energy between a	ll dimers.

Liquid crystal molecule	Conformation (LC+GP)	Interaction Energy (a.u.)	
CCH5	Parallel (armchair) Stacking	-17.8593	
P.P'-disubstituted diphenylacetylenes	Parallel (armchair) stacking	-17.8496	
5CB	Parallel (armchair) stacking	-17.8492	
PCH5	Parallel (armchair) stacking	-17.8479	
6O.5	Letter V shape	-17.8596	
7O.5	Parallel (armchair) stacking	-17.8507	
4-4' Disubstituted Biphenyls	Parallel (armchair) stacking	-17.8492	
MBA5	Parallel (armchair) stacking	-17.8514	
MBC5	Parallel (armchair) stacking	-17.8506	
H5CBP	Parallel (armchair) stacking	-17.8459	
5OCB	Parallel (armchair) stacking	-17.8467	

It was found that the LC-BLYP approach provides more stable energies for the LC-GP conformations, as shown in Table 13, than any of the dimers optimized using the other seven DFT methods. The greater stability of a dimer (LC+GP) is expressed by the least negative energy. Given that it displays the least negative energy when compared to the other DFT techniques listed in Table 13 and has acceptable - interaction goals, the LC-BLYP approach is appropriate for the LC and GP interaction energy

mechanism. Liquid crystals have many applications, including in liquid crystal displays (LCDs), liquid crystal thermometers, and mood rings. Liquid crystals can be used to create liquid crystal pixels, which are used in displays. Liquid crystals have been used in the development of new materials for energy investigations. Ongoing research focuses on the design, synthesis, characterization, and application of supramolecular and self-organizing liquid crystal systems and materials.

TABLE 13. Comparative interaction energies of dimers calculated using seven DFT methods.

11 BEE 13. Compared to interaction energies of anners calculated using seven B11 methods.								
Dimers\D FT Methods	M062X [40] (a.u.)	wB97XD [41] (a.u.)	Cam- B3LYP [42] (a.u.)	PBE1PBE [43] (a.u.)	M06 [44] (a.u.)	B3LYP [45] (a.u.)	LC-BLYP (a.u.) [46]	
P-P'-D-D	-6660.4625	-6660.5669	-6685.9076	-6655.2269	-6658.0045	-6662.6706	-6642.2641	
4-4'-D-B	-6750.5167	-6750.6121	-6748.9709	-6745.2197	-6748.0590	-6752.7458	-6732.2152	
5CB	-6562.0951	-6562.1851	-6560.5496	-6556.9320	-6559.6510	-6564.2628	-6544.1145	
70	-6913.4431	-6913.6208	-6911.8510	-6908.0167	-6910.9267	-6915.7616	-6894.5935	
CCH	-6569.2785	-6569.4369	-6567.7499	-6564.1317	-6566.8603	-6571.4774	-6551.2975	
60.2	-6874.1371	-6874.3065	-6872.5541	-6868.7442	-6870.3261	-6876.4409	-6855.3974	
H5CBP	-6712.4075	-6712.4988	-6710.8673	-6707.1394	-6709.9619	-6714.6211	-6694.2072	
MBA	-6866.1510	-6866.2695	-6864.6010	-6860.7716	-6863.6812	-6868.4251	-6847.6278	
MBC	-6730.6248	-6730.7233	-6729.0740	-6725.3404	-6728.1663	-6732.8562	-6712.3187	
5OCB	-6637.2445	-6637.3362	-6635.7048	-6632.0336	-6634.8025	-6639.4421	-6619.1634	
PCH	-6565.6852	-6565.8099	-6564.1500	-6560.5345	-6563.2605	-6567.8732	-6547.7126	

Conclusions

In this study, it was observed that the ionization potential and COSMO area decrease for all the dimers. Among the liquid crystals studied, only 6O.5 LC interacts with graphene in a V-shaped conformation, while all other LCs adopt a parallel stacking arrangement. The variations in COSMO area and COSMO volume indicate that the LCs adjust their structure in response to adsorption on graphene.

H5CBP LC transfers the most charge to graphene due to its high concentration of free ions, making it ideal for charge transfer 262

applications. In contrast, 6O.5 LC shows maximum positive energy in an armchair conformation, resulting in less favorable adsorption on graphene. Compared to 5OCB LC, H5CBP LC interacts more effectively with graphene because of the presence of an additional oxygen atom.

When comparing CCH5 LC, which contains two cyclohexane rings, with PCH5 LC, which has one benzene ring and one cyclohexane ring, the PCH5 LC shows stronger adsorption due to the π - π interactions of the benzene ring. In all dimers, the graphene sheet twists by

approximately 1.0 Å because the LC benzene rings exhibit π - π interaction at a distance of ~3.5, whereas the cyclohexane rings and terminal groups interact at a distance of ~ 2.5 Å without π stacking. Finally, nitrogen atom-based LCs interact actively with graphene but do not significantly increase the dipole moment, whereas oxygen atom-based LCs enhance the dipole of the dimer through their interaction with GP. Yet, GP interacts more actively with oxygen- and nitrogen-based LCs. While both oxygen- and nitrogen-based LCs contain the necessary dipole moments, the oxygen atombased LC dimers exhibit greater dipole moments compared to those with nitrogen atom-based LCs. Research is ongoing to design, synthesize, characterize, and apply supramolecular and selforganizing liquid crystal systems and materials.

Acknowledgments

We are very grateful to the Centre for Development of Advanced Computing (CDAC) for providing computational support for this work. We are also very thankful to Dr. Anakuthil Anoop Ayyappan (IIT KGP) for his assistance with computations. We are very thankful to Dr. Pawan Singh and Dr. Khem B. Thapa for the scientific discussion.

Funding Source: No funding was received for this work.

Conflict of Interest: The authors declare no conflicts of interest.

Data Availability Statement: Data will be made available upon reasonable request.

References

- [1] Novoselov, K.S., Geim, A.K., Morozov, S.V., Jiang, D.E., Zhang, Y., Dubonos, S.V., and Firsov, A.A., Sci., 306 (2004) 666.
- [2] Novoselov, K.S., Geim, A.K., Morozov, S.V., Jiang, D., Katsnelson, M.I., Grigorieva, I.V., and Firsov, A.A., Nat., 438 (2005) 197.
- [3] Geim, A.K., Science, 324 (2009) 1530.
- [4] Geim, A.K. and Novoselov, K.S., Nat. Mater., 6 (2007) 183.
- [5] Stoller, M.D., Park, S., Zhu, Y., An, J., and Ruoff, R. S., Nano Lett., 8 (2008) 3498.
- [6] Novoselov, K.S., Falko, V.I., Colombo, L., Gellert, P.R., Schwab, M.G., and Kim, K., Nat., 490 (2012) 192.
- [7] Xia, F., Mueller, T., Lin, Y.-M., Valdes-Garcia, A., and Avouris, P., Nat. Nano., (4) (2009) 839.
- [8] Geim, A.K. and Novoselov, K.S., Nat. Mat., 6 (2007) 183.
- [9] Mertens, R., "The Graphene Handbook", (Lulu.com, UK, 2018).
- [10] Basu, R. and Shalov, S.A., Phys. Rev. E, 96 (2017) 012702.
- [11] Shehzad, M.A., Tien, D.H., Iqbal, M.W., Eom, J., Park, J.H., Hwang, C., and Seo, Y., Sci. Rep., 5 (2015) 13331.
- [12] Yu, J.S., Yun, J.E., and Kim, J.H., Liq. Cryst., 40 (2013) 216.

- [13] Blake, P., Brimicombe, P.D., Nair, R.R., Booth, T.J., Jiang, D., Schedin, F., Ponomarenko, L.A., Morozov, S.V., Gleeson, H.F., Hill, E.W., Geim, A.K., and Novoselov, K.S., Nano Lett., 8 (2008) 1704.
- [14] Shen, Y. and Dierking, I., Appl. Sci., 9 (2019) 2512.
- [15] Mrukiewicz, M., Kowiorski, K., Perkowski, P., Mazur, R., and Djas, M., Beilstein J. Nanotechnol., 10 (2019) 71.
- [16] Fischer, S.A., Kołacz, J., Spillmann, C.M., and Gunlycke, D., Phy. Rev. E, 98 (2018) 052702.
- [17] Kumar, A., Ganguly, P., and Biradar, A.M., Liq. Cryst., 45 (11) (2018) 1620.
- [18] Frisch, M.J., Trucks, G.W., and Schlegel, H.B., "Gaussian 09", Revision A.02, (Gaussian, Inc., Wallingford CT, 2010).
- [19] Iikura, H., Tsuneda, T., Yanai, T., and Hirao, K., J. Chem. Phys., 115 (2001) 3540.
- [20] Lee, C., Yang, W., and Parr, R.G., Phys. Rev. B, 37 (1988) 785.
- [21] Hay, P.J. and Wadt, W.R., J. Chem. Phys., 82 (1985) 299.
- [22] Gresh, N., Claverie, P., and Pullman, A., Int. J. Quantum Chem., 16 (S13) (1979) 243.

[23] Dunmur, D.A. and Tomes, A.E., Mol. Cryst. Liq. Cryst., 97 (1983) 241.

- [24] Dunmur, D.A. and Toriyama, K., Liq. Cryst., 1 (1986) 169.
- [25] Malthete, J., Leclercq, M., Dvolaitzky, M., Gabard, J., Billard, J., Pontikis, V., and Jacques, J., Mol. Cryst. Liq. Cryst., 23 (1973) 233.
- [26] Breddels, P.A. and Mulkens, J.C.H., Mol. Cryst. Liq. Cryst., 147 (1987) 107.
- [27] Coles, H.J. and Sefton, M.S., Mol. Cryst. Liq. Cryst., 3 (1986) 63.
- [28] Coles, H.J. and Sefton, M.S., Mol. Cryst. Liq. Cryst., 4 (1987) 123.
- [29] Siedler, L.T.S., Hyde, A.J., Pethrick, R.A., and Leslie, F.M., Mol. Cryst. Liq. Cryst., 90 (1983) 255.
- [30] Bock, F.-J., Kneppeand, H., and Schneider, F., Liq. Cryst., 1 (1986) 239.
- [31] Kneppe, H., Schneider, F., and Sharma, N.K., J. Chem. Phys., 77 (1982) 3203.
- [32] Gray, G.W., Harrison, K.I., and Nash, J.A., Elec. Lett., 9 (6) (1973) 130.
- [33] Pohl, L., Eidenschink, R., Krause, G., and Erdmann, D., Phys. Lett. A, 60 (1977) 421.
- [34] Sen, S., Kali, K., Roy, S.K., and Roy, S.B., Mol. Cryst. Liq. Cryst., 126 (1985) 269.
- [35] Finkenzeller, U., Geelhaar, T., Weber, G., and Pohl, L., Liq. Cryst., 5 (1989) 313.

- [36] Abdoh, M.M.M., Shivaprakash, S.N.C., and Prasad, J.S., J. Chem. Phys., 77 (1982) 2570.
- [37] Pestev, S. and Vill, V., "Physical Properties of Liquid Crystals", In: "Landolt-Börnstein", 5A, (Group VIII Advanced Materials and Technologies, Springer, 2003).
- [38] Rao, P.B., Potukuchi, D.M., Murthy, J.S.R., Rao, N.V.S., and Pisipati, V.G.K.M., Cryst. Res. Technol., 27 (1992) 839.
- [39] Hardouin, F. Gasparoux, H., and Delhaes, P., J. Phys. Colloquies, 36 (1975) C1.
- [40] Rao, N.V.S., Pisipati, V.G.K.M., Sankar, Y.G., Potukuchi, D.M., Phase Transit., 7 (1986) 49.
- [41] Dubois, J.C. and Zann, A., J. Phys. Symp., 37 (1976) C3.
- [42] Leenhouts, F., de Jeu, W.H., and Dekker, A.J., J. Phys., 40 (1979) 989.
- [43] Pisipati, V.G.K.M. and Rao, N.V.S.Z., Naturforsch., 39a (1984) 696.
- [44] Zugenmaier, P. and Heiske, A., Liq. Cryst., 15 (6) (1993) 835.
- [45] Basu, R., Kinnamon, D., and Garvey, A., Liq. Cryst., 43 (13-15) (2016) 2375.
- [46] Ali, I., Sharma, S., and Bezbaruah, B., Computat. Chem., 6 (2018) 71.